IAI
Journals.ASM.org

Involvement of Host Cell Integrin α2 in *Cryptosporidium parvum* Infection

Haili Zhang,[a] Fengguang Guo,[a] and Guan Zhu[a,b]

Department of Veterinary Pathobiology, College of Veterinary Medicine & Biomedical Sciences, Texas A&M University, College Station, Texas, USA,[a] and Faculty of Genetics Program, Texas A&M University, College Station, Texas, USA[b]

***Cryptosporidium parvum* is an opportunistic pathogen in AIDS patients. It is an intracellular but extracytoplasmic parasite residing in a host cell-derived parasitophorous vacuole. It is still poorly understood how this parasite interacts with host cells. We observed that expression of the integrin α2 (ITGA2) gene in host cells was significantly upregulated upon *C. parvum* infection, and a higher level of ITGA2 protein was present in the parasite infection sites. The infection could be reduced by the treatment of antibodies against ITGA2 and integrin β1 (ITGB1) subunits, as well as by type I collagen (an integrin α2β1 ligand). We also generated stable knockdown of ITGA2 gene expression in HCT-8 cells and observed consistent reduction of parasite infection in these knockdown cells. Collectively, our evidence indicates that host cell ITGA2 might be involved in interacting with *Cryptosporidium* during infection, probably acting as part of the regulatory elements upstream of the reported recruiting and reorganization of F actin at the infection sites.**

Cryptosporidium parvum is an apicomplexan parasite infecting both humans and animals (30, 31, 36). It is also an AIDS opportunistic pathogen, for which treatment is currently unavailable (9). Like other apicomplexans, *Cryptosporidium* possesses a complex life cycle that starts with the ingestion of oocysts, followed by excystation in the intestine to release sporozoites that invade host gastric or intestinal epithelial cells. During intracellular development, *Cryptosporidium* resides within a host cell-derived membrane, the parasitophorous vacuole membrane (PVM). The PVM-contained parasite is connected to the host cell cytosol only by an electron-dense juncture, rather than residing within host cell cytoplasm. Therefore, *Cryptosporidium* is considered an intracellular but extracytoplasmic parasite which differs from the majority of other intracytoplasmic apicomplexans.

Although morphology at the parasite infection site has been extensively studied, very limited knowledge on how the parasite interacts with host cell molecules has accumulated. Several *C. parvum* membrane proteins and antigens that might be involved in the interaction with host cells have been reported. These include various mucin-like proteins, thrombospondin-related adhesive proteins (TRAPs), and circumsporozoite-like antigen/ligand (CSL) (5, 26, 32). It is known that host cell F actin is reorganized and accumulates underneath the electron-dense membrane structure (13, 14). Using biliary epithelial cells as a model of cryptosporidial infection, several host cell factors and pathways have been shown to possibly be involved in the remodeling of F actin, including c-Src-dependent tyrosine phosphorylation for the accumulation of cortactin and phosphatidylinositol-3-kinase (PI3K) and frabin-mediated activation of CDC42 for the recruitment of Neural Wiskott-Alrich syndrome protein (WASP) (7, 8, 10). However, the upstream elements within the pathways, as well as the host cell membrane proteins that may interact directly with the parasite during invasion and development, have yet to be defined.

Integrins (ITGs) are a family of surface receptors associated with extracellular matrix (ECM) complexes. These receptors consist of α and β subunits. Each subunit has several isoforms that form up to 24 prototypes of αβ heterodimers in higher vertebrates (2, 3, 17–20). ITGs in the cytoplasmic membrane are involved in the transduction of both outside-in and inside-out signals to regulate cell polarity, migration, growth, survival, and differentiation (11, 20, 22, 28). One important function of ITGs is to regulate the dynamics and reorganization of actins at the sites of adhesion via a matrix of proteins and pathways, such as the FAK/Src, PI3K, ILK, Rho, and Rac proteins and the Cdc42-WASP-Arp2/3 pathway (23).

In the present study, we observed that the expression of integrin α2 (ITGA2) in human cells was upregulated upon infection by *C. parvum* and ITGA2 protein was recruited to the sites of infection. We have confirmed that infection could be reduced by the knockdown of ITGA2 expression in host cells and by treatment using antibodies specific to ITGA2 and the ligand type I collagen (collagen-I). These observations indicate that host cell ITGA2 may be involved in the interaction with cryptosporidial infection.

MATERIALS AND METHODS

Parasite and *in vitro* cultivation. Fresh oocysts of *C. parvum* (Iowa strain) were purchased from Bunch Grass Farm (Deary, ID). Oocysts were further purified by a Percoll-based gradient centrifugation method and surface sterilized with 10% bleach for 7 min on ice, followed by washes with phosphate-buffered saline (PBS), as described previously (1, 6, 25). A human ileocecal epithelial cell line (HCT-8, ATCC CCL-244) was used to assay cryptosporidial infection and to generate stable ITGA2-knockdown (KD) cells. HCT-8 cells were maintained as described previously (6). In a typical infection assay, HCT-8 and ITGA2-KD cells were seeded into 24-well plates and allowed to grow overnight until they reached ~80% confluence. Oocysts (less than 3 months old) were suspended in the same

Received 25 August 2011 Returned for modification 13 October 2011
Accepted 10 February 2012
Published ahead of print 21 February 2012
Editor: J. F. Urban, Jr.
Address correspondence to Guan Zhu, gzhu@cvm.tamu.edu.
Supplemental material for this article may be found at http://iai.asm.org/.

doi:10.1128/IAI.05862-11

culture medium and added to plates with specified parasite/host cell ratios as described below. Cells receiving no infection or sham infection with oocysts heat killed by pretreatment at 65°C for 30 min were included as controls. Uninfected controls received the same treatments as experimental groups. After incubation for 3 h to allow parasite excystation and invasion, uninfected parasites were removed by a medium exchange. At this stage at 3 h postinfection, cells might be harvested to determine the level of parasite invasion or allowed to grow further for a total of 8 to 18 h to determine the effects of described conditions on early intracellular development of the parasite. The selection of these time points was mainly to restrict the parasite growth within the first cell cycle (i.e., first merogony development), before the release of merozoites that might occur at ~20 to 24 h postinfection. The release of merozoites would damage and trigger apoptosis in host cells, and the unsynchronized second parasite cell cycle by the released merozoites (i.e., second merogony) in a mixture of damaged and healthy cells would also complicate the study of host cell-parasite molecular interactions. It was also noticed that ITGA2-KD cells might gradually increase the expression of ITGA2 upon parasite infection, particularly after >8 h of infection (see below for details).

Effects of integrin antibodies and ligand collagen-I on parasite infection. Monoclonal antibody (MAb) against ITGA2 (clone C-9) was purchased from Santa Cruz Biotechnology (Santa Cruz, CA). Additional MAbs against β1 (6S6), α6 (NKI-GoH3), β4 (ASC-3), α3 (P1B5), β3 (B3A), and αvβ3 (23C6) subunits were purchased from Millipore (Billerica, MA). Integrin α2β1 ligand collagen-I was purchased from Sigma-Aldrich (St. Louis, MO). HCT-8 cell monolayers in 24-well plates were preincubated with MAbs or collagen-I for 1 h prior to the addition of *C. parvum* oocysts. The final concentration of each antibody and ligand was 10 μg/well. Host cells were infected with live or heat-killed sham parasite with an oocyst/host cell ratio at 1:5. Cells were washed with RNase-free PBS 3 times and harvested at 3 h and 18 h after infection for the isolation of total RNA and detection of parasite load by quantitative reverse transcription (RT)-PCR (qRT-PCR), as described below.

Generation of stable ITGA2-KD cells. Stable ITGA2-KD cells were generated by small hairpin RNA (shRNA)-based methods. SureSilencing shRNA vector for human ITGA2 (catalog no. KH00625N) and a negative-control vector containing only a scrambled artificial sequence not matching any human gene sequences were purchased from SABiosciences (now part of Qiagen Inc., Frederick, MD). HCT-8 cells with ~80% confluence in 24-well plates were transfected with shRNA plasmids (0.8 μg/well), using a Lipofectamine protocol recommended by the manufacturer. After 24 to 48 h posttransfection, cells were replated to a low density at <10% confluence in culture medium containing 580 μg/ml neomycin that was exchanged every 2 to 3 days. Cells were replated every week for 2 weeks. Monoclonal populations were obtained by diluting cells to ~1 cell/400 μl and plating them into 96-well plates at 200 μl/well. Cells were allowed to form large colonies, and wells containing single colonies were selected and maintained in medium containing 300 μg/ml neomycin.

Western blot analysis of ITGA2 protein in WT and KD cells. Cultured wild-type (WT) and ITGA2-KD cells were removed from plates with a cell scraper and lysed in radioimmunoprecipitation assay (RIPA) buffer containing a protease inhibitor cocktail for mammals (Sigma-Aldrich). Total protein concentrations were determined by the Bradford method. Protein lysates (20 μg/lane) were separated by 7% SDS-PAGE and transferred onto nitrocellulose membranes. The blots were treated with 5% bovine serum albumin (BSA) in 10 mM Tris-HCl (pH 7.5) containing 166 mM NaCl and 0.05% Tween 20 (5% BSA-TBST) and incubated with anti-ITGA2 MAb (1:200 dilution in 5% BSA-TBST) and then horseradish peroxidase (HRP)-conjugated goat anti-mouse IgG antibody (1:5,000 dilution). Each incubation step was carried out for 1 h at room temperature, followed by 3 washes in TBST. Human glyceraldehyde-3-phosphate dehydrogenase (GAPDH) was detected with MAb (1:1,000 dilution; Millipore) as a loading control. Antibody-labeled blots were visualized using an enhanced chemiluminescence (ECL) reagent (Sigma-Aldrich).

Detection of parasite growth *in vitro* and gene expressions by qRT-PCR. Total RNA was isolated from HCT-8 or ITGA2-KD cells uninfected or infected with *C. parvum* for various times using an RNeasy minikit (Qiagen Inc., Valencia, CA). Cell monolayers were gently washed 3 times with nuclease-free PBS and lysed in 350 μl of lysis buffer by incubating cells at 37°C for 20 min, followed by gentle pipetting at least 20 times through 200-μl pipetting tips. Samples were treated with RNase-free DNase (Qiagen Inc., Valencia, CA) to remove DNA, according to the manufacturer's protocol. The quality and purity of RNA were determined using a NanoDrop ND-1000 spectrophotometer at 260/280 nm (NanoDrop Technologies, Wilmington, DE). A Qiagen one-step RT-PCR QuantiTect SYBR green RT-PCR kit was employed to evaluate both gene expression levels and parasite growth as described below. Each 25-μl reaction mixture contained 2 ng total RNA, 500 nM each primer, 10 nM fluorescein isothiocyanate (FITC), 0.25 μl RT master mix, and 1× QuantiTect SYBR green. The mixtures were incubated at 50°C for 30 min to synthesize cDNA, heated at 95°C for 15 min to inactivate the reverse transcriptase, and then subjected to 40 thermal cycles of PCR amplification (95°C for 20 s, 58°C for 30 s, and 72°C for 30 s) with an iCycler iQ real-time PCR detection system (Bio-Rad Laboratories, Hercules, CA). At least 2 replicate qRT-PCRs were performed for each sample. All reagents for the qRT-PCR were loaded manually.

After host cells had been infected for 3 and 8 h (oocyst/host cell ratio, 1:20), parasite growth in HCT-8 and ITGA2-KD cells was assayed by detecting parasite 18S rRNA levels using primers Cp18S-1011F (5′-TTGTTCCTTACTCCTTCAGCAC-3′) and Cp18S-1185R (5′-TCCTTCCTATGTCTGGACCTG-3′) as described previously (6). Human 18S rRNA levels were detected using primers Hs18S-1F (5′-GGCGCCCCCTCGATGCTCTTA-3′) and Hs18S-1R (5′-CCCCCGGCCGTCCCTCTTA-3′) for evaluating host cell integrity and for normalization (6). The relative levels of human ITG subunit transcripts in WT and ITGA2-KD cells were determined by qRT-PCR using the following primer pairs, which were designed using the Primer3Plus server (http://www.bioinformatics.nl/cgi-bin/primer3plus/primer3plus.cgi) (33) and validated by BLAST searches against the NCBI nucleotide databases (http://blast.ncbi.nlm.nih.gov/Blast.cgi): 5′-AGGACGGACTTTGCATTTCTGAT-3′ and 5′-CCACCTGGCATGTTACTTCTGT-3′ for α2 (ITGA2), 5′-GTGCAAATCCCACAACACTG-3′ and 5′-TTTCAATAGTCCAGGAAGAAAAGG-3′ for β1, 5′-AAGGCTCCTGTTTTGCACAG-3′ and 5′-ATGTAAGTCAGCCACGCCA-3′ for α6, and 5′-CCCGCCACGTCCCACTAG-3′ and 5′-TTTTTTTAGCAGTAGCAAAACCA-3′ for β4. All experiments were performed at least in triplicate for each experimental condition. Relative levels of gene expression were calculated by a $\Delta\Delta C_T$ method with a general formula of $2^{-\Delta\Delta CT}$, in which changes in threshold cycle (ΔC_T) values between specified gene transcripts and human 18S rRNA were first determined by the equation $C_{T[\text{gene}]} - C_{T[18S\ \text{rRNA}]}$, followed by the calculation of $\Delta\Delta C_T$ between KD and WT cells or between treated and untreated samples. Statistical significance on the relative levels of gene expression and on the parasite infections was examined by Student's *t* test.

Immunofluorescence microscopy of ITGA2 protein in infected cells. The same quantities of ITGA2-KD (KD137-2-3) and a negative-control (NC) vector containing a scrambled sequence (NC1-2) cells were seeded into 24-well plates containing coverslips and allowed to grow to ~80% confluence. Cells were infected with *C. parvum* (oocyst/host cell ratio, 2:1) for 3 h and 18 h and then fixed in PBS-buffered paraformaldehyde (3.7%) for 30 min. After 3 washes in PBS, excess paraformaldehyde was quenched with 50 mM NH_4Cl for 15 min. Fixed cells on coverslips were washed and permeabilized with 0.1% Triton X-100 and 0.05% SDS in PBS for 5 min, washed in 5% fetal bovine serum (FBS)-PBS 3 times (5 min each), and then incubated with anti-ITGA2 MAb (4 μg/ml in 5% FBS-PBS) for 1 h. After 3 washes in PBS, cells were incubated with Alexa 594-labeled goat anti-mouse IgG antibody diluted 1:1,000 in PBS for 45 min, washed 3 times with PBS, and then mounted on glass microscopy slides with a SlowFade kit containing 4′,6-diamidino-2-phenylindole (DAPI) for counterstaining of nuclei (Molecular Probes/Invitrogen).

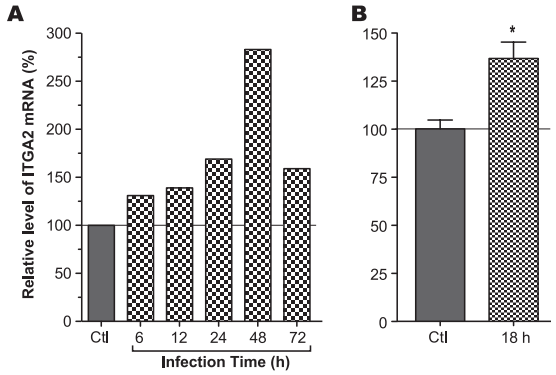

FIG 1 Upregulated human ITGA2 gene expression in HCT-8 cells upon infection with *C. parvum*. (A) Relative levels of ITGA2 transcripts based on data extracted from an earlier microarray analysis with NCBI Gene Express Omnibus data sets (accession number GSE2077; http://www.ncbi.nlm.nih.gov/geo/query/acc.cgi?acc=GSE2077) (12); (B) relative levels of ITGA2 transcripts in uninfected control (Ctl) cells and those infected with *C. parvum* for 18 h, as determined by qRT-PCR in this study. The transcript levels were first normalized with those of host cell 18S rRNA and then displayed relative to those in uninfected cells. *, $P < 0.05$ by Student's *t* test versus uninfected control.

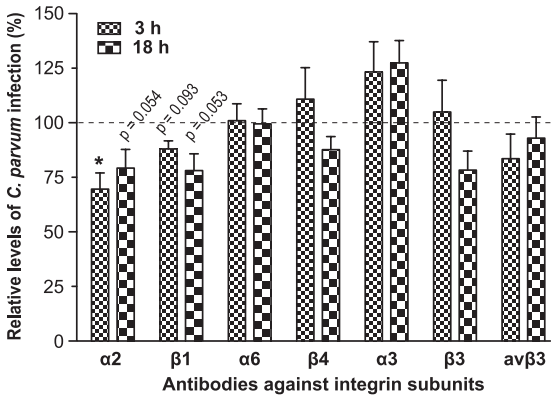

FIG 2 Effects of treatment by antibodies against various integrin subunits on the infection of *C. parvum* in HCT-8 cells. A significant reduction in infection was observed in the group treated with anti-integrin $\alpha 2$ antibodies in 3-h infection assays. Bars represent standard errors of the means derived from triplicate treatments. *, $P < 0.05$ by Student's *t* test versus untreated control cells.

Cells labeled with fluorescent molecules were examined with an Olympus BX51 research microscope equipped with appropriate filter sets (i.e., excitation at 510 to 550 nm with a 590-nm barrier filter for Alexa 594 and excitation at 330 to 385 nm with a 420-nm barrier filter for DAPI). Images captured under the same exposure parameters with a Retiga SRV charge-coupled-device digital camera (QImaging) were used for comparison of fluorescence intensity among different samples.

RESULTS

The expression of the host cell ITGA2 gene was upregulated upon *C. parvum* infection. We observed from published microarray data that the ITGA2 gene expressed in HCT-8 cells was consistently upregulated at various time points upon *C. parvum* infection (Fig. 1A) (12). Similar results were also obtained in Caco-2 cells infected with *C. parvum* for 18 h in our unpublished analysis using Affymetrix U133A microarrays (i.e., 40% increase; $P = 0.00296$). These observations were further validated by qRT-PCR in HCT-8 cells inoculated with *C. parvum* oocysts for 18 h, in which the levels of ITGA2 transcripts were increased by 37% (Fig. 1B).

Antibody specific to ITGA2 and its ligand, collagen-I, could reduce *C. parvum* infection. To determine whether ITGA2 was involved in *C. parvum* infection, we treated HCT-8 cells with MAbs against ITGA2 and 6 other subunits (i.e., $\beta 1$, $\alpha 6$, $\beta 4$, $\alpha 3$, $\beta 3$, and $\alpha v\beta 3$) to test their effects on parasite invasion and growth *in vitro*. Among them, antibodies to $\alpha 2$ and $\beta 1$ consistently inhibited the parasite growth by ~20% to 30% in both 3-h and 18-h infection assays, with *P* values being below (3 h, $\alpha 2$) or near (the other three groups) 0.05%, whereas all other antibodies except for the $\alpha 3$ antibody had either no or little effect on parasite infection (Fig. 2). On the other hand, antibody against $\alpha 3$ promoted both invasion and intracellular development by 24% and 28%, respectively.

Because collagen-I is a known ECM ligand for the ITG $\alpha 2\beta 1$ complex (3, 29), we also examined the effect of this ligand on *C. parvum* infection in HCT-8 cells. When soluble collagen-I was added to the culture, only a slight reduction of parasite invasion (6%) was observed in the 3-h infection assay. However, a significant reduction of intracellular development (32% and 28%, respectively) was detected in the 12-h and 18-h infection assays (Fig. 3). These data suggest that collagen-I might play a more important role for the intracellular development of the parasite rather than for invasion, probably via acting as a critical ECM component connecting ITGA2 and parasite at the host cell-parasite juncture.

Stably transfected HCT-8 cells could be generated to silence ITGA2 gene expression at varied levels. We developed stable transfection of serially cloned ITGA2-KD cell lines derived from HCT-8 cells to test the effect of reduced ITGA2 expression on *C. parvum* infection. In comparison with WT cells, the levels of ITGA2 mRNA in various ITGA2-KD lines were reduced from 16% to 96%, whereas no or few changes were observed in the negative-control cells (NC1-2), as determined by qRT-PCR (Fig. 4A). The gene silencing was further validated by Western blot analysis, in which ITGA2 protein was clearly detectable in the WT and NC1-2 controls but undetectable in three ITGA2-KD lines that displayed the highest reduction in ITGA2 expression (i.e., KD137-1-4, KD137-2-3, and KD137-1-6) (Fig. 4A, inset).

We also examined the effect of ITGA2 knockdown on the expression of three other integrin subunits (i.e., $\beta 1$, $\alpha 6$, and $\beta 4$) among select ITGA2-KD cell lines and observed a general pattern. In comparison with NC1-2 controls, the expression of $\beta 1$, $\alpha 6$, and

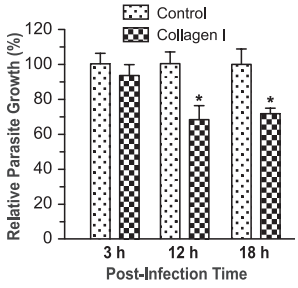

FIG 3 Effects of collagen-I on *C. parvum* infection. Treatment of HCT-8 cells by collagen-I significantly reduced the infection by *C. parvum*, as determined by qRT-PCR detection of parasite 18S rRNA levels in the 12-h and 18-h infection assays. Levels of infection were expressed relative to the untreated control. Bars represent standard errors of the means derived from triplicate treatments. *, $P < 0.05$ by Student's *t* test versus untreated control cells.

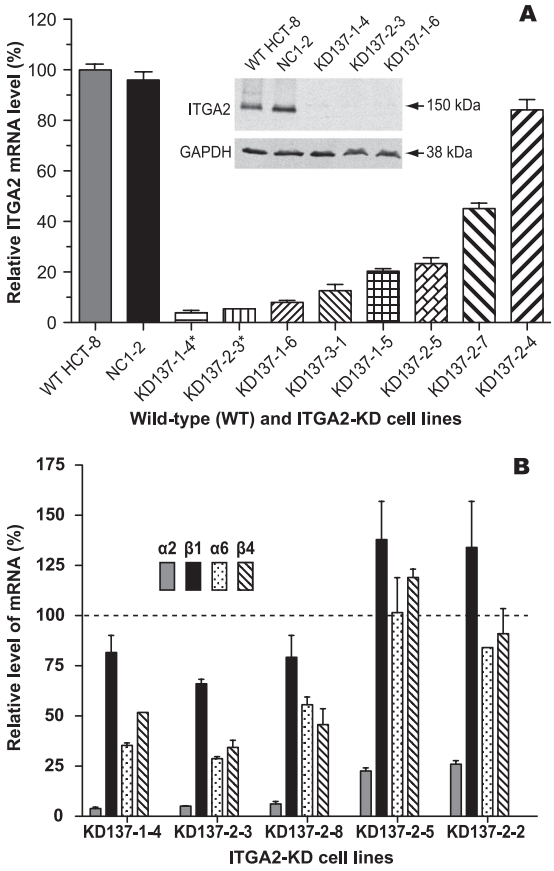

FIG 4 Gene expression profiles in ITGA2-KD cells. (A) Relative expression levels of host ITGA2 mRNA and protein (inset) in various control and ITGA2-KD cells, as determined by qRT-PCR and Western blot analysis. GAPDH was used as a protein load control. (B) Levels of gene expression of four different integrin subunits in select ITGA2-KD lines, as determined by qRT-PCR, relative to those in WT HCT-8 cells. The ITGA2-KD lines marked with asterisks were used in subsequent infection assays. Bars represent standard errors of the means derived from biological triplicates. WT, wild-type HCT-8 cell line; NC1-2, negative-control vector with a scrambled sequence.

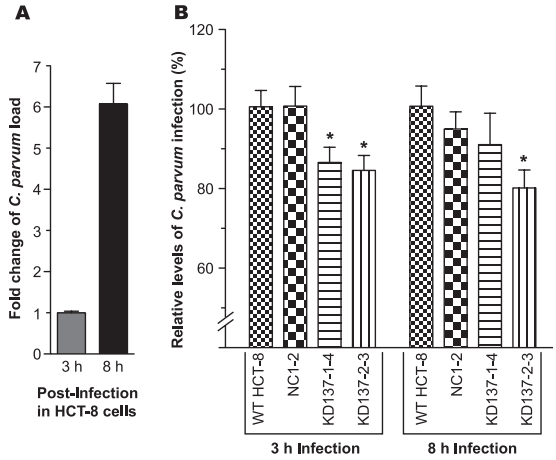

FIG 5 Levels of *C. parvum* infection in control and ITGA2-KD cell lines. (A) The rapid growth of *C. parvum* in the early stage of infection in HCT-8 cells determined by qRT-PCR. A 6-fold increase of parasite 18S rRNA levels was observed during the period from 3 h to 8 h postinfection. (B) The infection of *C. parvum* was significantly decreased in two ITGA2-KD cell lines (KD137-1-4 and KD137-2-3) in comparison to those in WT and negative-control (NC1-2) cells in both 3-h and 8-h infection assays. Bars represent standard errors of the means derived from triplicate treatments. *, $P < 0.05$ by Student's *t* test versus *C. parvum*-infected WT control.

β4 integrins was significantly downregulated in ITGA2-KD cells that had the lowest ITGA2 expression levels (i.e., in KD137-1-4, KD137-2-3, and KD137-2-8 cells, which showed >95% reductions in ITGA2 expression levels) but either upregulated or only slightly downregulated in cells with relatively higher levels of ITGA2 expression (i.e., in KD137-2-5 and KD137-2-2 cells, which showed ~75% reductions) (Fig. 4B).

In comparison with the control cells, ITGA2-KD cells did not show much difference in cell adhesion and growth during the first 6 to 12 h of growth after seeding. However, the morphological difference between the negative-control and ITGA2-KD cells was more obvious from 12 h to 48 h after seeding. The KD cells generally displayed more round or clustered shapes than vector-control cells (see Fig. S1 in the supplemental material), which may indicate a migration defect in knockdown cells. Surprisingly, however, at 24 to 48 h after seeding, ITGA2-KD cells showed an ~25% higher growth rate than negative-control cells (see Fig. S2 in the supplemental material). Flow cytometric analysis of cells double stained with propidium iodide and annexin V–FITC indicated no statistically significant differences in the ratios of dead or apoptotic cells between the WT, NC1-2, KD137-1-4, and KD137-2-3 cell lines (see Fig. S3 in the supplemental material), suggesting that apoptosis had no or little effect on the subsequent parasite infection assays.

***Cryptosporidium* early infection was reduced in ITGA2-KD cells.** Two ITGA2-KD cell lines with the lowest level of ITGA2 expression (KD137-1-4 and KD137-2-3) were used to test the effect of knockdown on parasite infection by an 18S rRNA-based qRT-PCR method. *C. parvum* was allowed to infect WT and KD cells for 3 and 8 h to represent parasite invasion and early stages of intracellular development. There was an approximately 6-fold increase in the level of *C. parvum* 18S rRNA (Cp18S) from 3 h to 8 h of infection in WT cells (Fig. 5A), suggesting a rapid parasite growth in the early stage of intracellular development. In comparison with WT cells, both parasite invasion (3 h infection) and early intracellular development (8 h infection) were moderately but consistently reduced by ~15% to 20% in the two ITGA2-KD cell lines (Fig. 5B). On the other hand, no changes or only a slight reduction was observed in negative-control NC1-2 cells (Fig. 5B). Data on the parasite growth for 18 h in KD cells were inconclusive, as they varied greatly between experiments, although there was a general tendency for a reduction of parasite growth in KD137-2-3 cells but not in KD137-1-4 cells (data not shown). This is probably due to the significant rebound of ITGA2 mRNA levels from ~5% back to ~40% in both KD cell lines (in comparison with those in WT and NC1-2 cells) upon parasite infection for 18 h (Fig. 6).

ITGA2 protein was recruited to the *C. parvum* infection sites at the parasite intracellular development stage. In addition to the increased level of ITGA2 transcripts of host cells in response to *C. parvum* infection, we also observed that ITGA2 was recruited to the infection sites during parasite intracellular development (Fig. 7). Immunofluorescence microscopy using anti-ITGA2 MAb indicated that this protein was more concentrated at the infection sites in both the 3-h and 18-h assays. To our surprise,

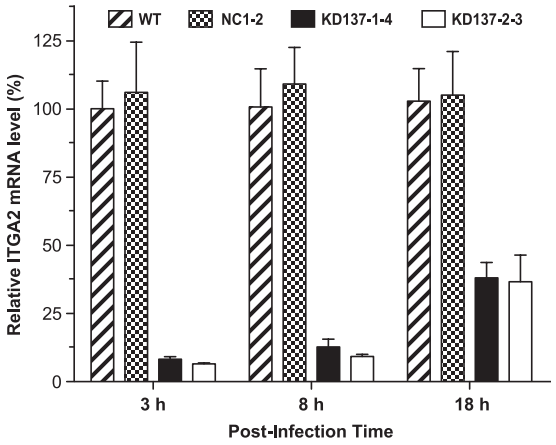

FIG 6 Significant rebound of ITGA2 gene expression in knockdown (KD) cell lines upon infection by *C. parvum* determined by qRT-PCR.

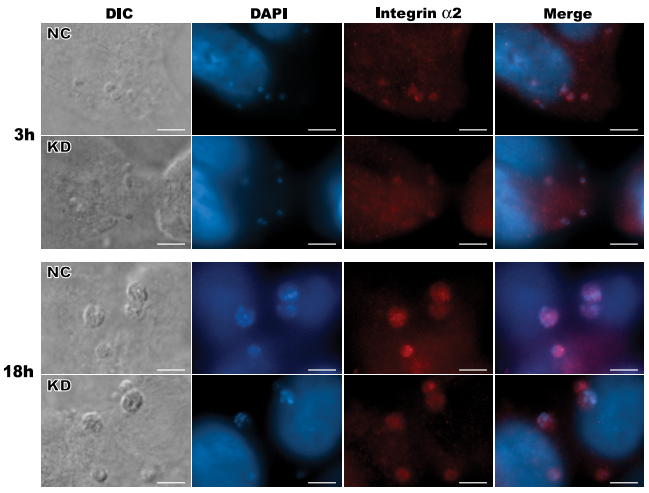

FIG 7 ITGA2 protein was recruited to the infection sites in vector-control NC1-2 (NC) and KD137-1-4 (KD) cells infected with *C. parvum* for 3 h and 18 h, respectively, as determined by immunofluorescence microscopy. DIC, differential inference contrast; DAPI, 4′,6-diamidino-2-phenylindole for counterstaining of nuclei; Integrin α2, Alexa 594-labeled integrin α2 protein; Merge, DAPI-stained nuclei and Alexa 594-labeled α2 protein. Bars, 5 μm.

however, ITGA2 proteins were also detectable at the infection sites in ITGA2-KD cells with a fluorescence signal intensity comparable to that in the control cells (Fig. 7, marked KD), indicating the presence of a small but adequate amount of ITGA2 protein in these knockdown cells. Nonetheless, the presence of ITGA2 protein in KD cells was consistent with the rebound of ITGA2 gene expression in KD cells upon infection for 18 h, as described above (Fig. 6).

DISCUSSION

It is known that a number of intracellular microbial pathogens could directly or indirectly exploit ITGs and associated pathways to breach the host cell surface barrier (4, 15, 16, 21). Some pathogens might bind to the host cell ITGs with their special outer membrane proteins (21), while others may interact with host ITGs via ECM proteins, which serve as receptors for pathogen adherence and internalization (4). More recently, the ITG $\alpha2\beta1$ complex was also reported to mediate the entry of *Bacillus anthracis* spores into epithelial cells (34). Our observations provide evidence to also support the involvement of ITGA2 in *C. parvum* infection based on the following: (i) host cell ITGA2 gene expression was significantly upregulated upon infection in both WT and KD cells, (ii) ITGA2 was recruited to the parasite infection sites in cultured host cells, and (iii) parasite invasion and intracellular development were reduced in ITGA2-KD cells and by its specific MAbs and its ligand, type I collagen.

Although the observed effects in parasite infections by antibody and ligand treatments, as well as by gene knockdown, were at most moderate (Fig. 2, 3, and 5), the reductions were consistent with *P* values of less than or near 0.05%. These moderate effects imply that ITGA2 is involved in parasite infection but its role might be noncritical, or it might be critical but the effect could not be fully assessed by a gene-knockdown approach, as it is unable to completely eliminate the expression of ITGA2. We observed the presence of ITGA2 at the infection sites in ITGA2-KD cells (Fig. 6), despite the fact that its protein level was undetectable by Western blot analysis (Fig. 4A). These observations suggest that although the ITGA2 mRNA level in these KD cells was reduced by >95% and the ITGA2 protein level was below the sensitivity of Western blot detection, a very small amount of ITGA2 protein was still present and could be recruited to the infection sites. Additionally, the apparent rebound of ITGA2 mRNA levels in KD cells upon relatively long parasite infection, as shown in Fig. 6, is also attributed to the synthesis of even more ITGA2 proteins. Therefore, a complete deletion/knockout of the ITGA2 gene in HCT-8 cells may be needed to ultimately test the necessity of ITGA2 in *Cryptosporidium* infection. Additionally, it is possible that other ITG subunits might also interact with the parasite during its infection and intracellular development, thus compensating for the loss of ITGA2 in the ITGA2-KD cells. On the other hand, the observed rebound of ITGA2 expression further supports the notion that ITGA2 expression is upregulated upon *C. parvum* infection.

ITGA2 typically forms a heterodimer with the $\beta1$ subunit ($\alpha2\beta1$). Our current data show that antibody against the $\beta1$ subunit could also inhibit parasite infection (Fig. 2), which is well correlated with the reduction of parasite infection in ITGA2-KD cells and by anti-ITGA2 antibody treatment. It is known that ITGs not only are capable of directly anchoring actin filaments on the cytosolic side of the cytoplasmic membrane but also are able to regulate F-actin remodeling via the FAK/Src/CDC42-associated signal transduction pathway (24, 27, 29). On the other hand, it has been reported that host cell c-Src-dependent tyrosine phosphorylation and PI3K-mediated activation of CDC42 are involved in interactions with parasite infection via regulation of the recruitment of F actin at the host-parasite interface (7, 8, 10). Collectively, albeit further investigations are needed to make firm conclusions, we speculate that ITGs may act at the upstream level to regulate the F-actin remodeling via the FAK/Src/CDC42 pathway.

The HCT-8 cell line is commonly used to study cryptosporidial infection and test drug efficacies *in vitro* (6). However, except for a transient gene expression knockdown with microRNA (35), stable knockdown of gene expression was unreported. This is the first time that a stable gene knockdown has been obtained for HCT-8 cells, showing that shRNA-based gene knockdown could be applied to this cell line to study the roles of other genes of interest on infection by *C. parvum* or other pathogens.

ACKNOWLEDGMENTS

We thank Beiyan Zhou and Guoqing Zhuang for their technical assistance in the flow cytometric analysis and Jason M. Fritzler for his critical reading of the manuscript.

This study was supported by a grant from the National Institutes of Health (NIH), National Institute of Allergy and Infectious Diseases (NIAID) (R21 AI80022 to G.Z.).

REFERENCES

1. **Arrowood MJ, Sterling CR.** 1987. Isolation of *Cryptosporidium* oocysts and sporozoites using discontinuous sucrose and isopycnic Percoll gradients. J. Parasitol. **73**:314–319.
2. **Banno A, Ginsberg MH.** 2008. Integrin activation. Biochem. Soc. Trans. **36**:229–234.
3. **Barczyk M, Carracedo S, Gullberg D.** 2010. Integrins. Cell Tissue Res. **339**:269–280.
4. **Bergmann S, et al.** 2009. Integrin-linked kinase is required for vitronectin-mediated internalization of *Streptococcus pneumoniae* by host cells. J. Cell Sci. **122**:256–267.
5. **Borad A, Ward H.** 2010. Human immune responses in cryptosporidiosis. Future Microbiol. **5**:507–519.
6. **Cai X, Woods KM, Upton SJ, Zhu G.** 2005. Application of quantitative real-time reverse transcription-PCR in assessing drug efficacy against the intracellular pathogen *Cryptosporidium parvum* in vitro. Antimicrob. Agents Chemother. **49**:4437–4442.
7. **Chen XM, et al.** 2003. *Cryptosporidium parvum* invasion of biliary epithelia requires host cell tyrosine phosphorylation of cortactin via c-Src. Gastroenterology **125**:216–228.
8. **Chen XM, et al.** 2004. Cdc42 and the actin-related protein/neural Wiskott-Aldrich syndrome protein network mediate cellular invasion by *Cryptosporidium parvum.* Infect. Immun. **72**:3011–3021.
9. **Chen XM, Keithly JS, Paya CV, LaRusso NF.** 2002. Cryptosporidiosis. N. Engl. J. Med. **346**:1723–1731.
10. **Chen XM, et al.** 2004. Phosphatidylinositol 3-kinase and frabin mediate *Cryptosporidium parvum* cellular invasion via activation of Cdc42. J. Biol. Chem. **279**:31671–31678.
11. **Damsky CH, Ilic D.** 2002. Integrin signaling: it's where the action is. Curr. Opin. Cell Biol. **14**:594–602.
12. **Deng M, Lancto CA, Abrahamsen MS.** 2004. *Cryptosporidium parvum* regulation of human epithelial cell gene expression. Int. J. Parasitol. **34**: 73–82.
13. **Elliott DA, Clark DP.** 2000. *Cryptosporidium parvum* induces host cell actin accumulation at the host-parasite interface. Infect. Immun. **68**: 2315–2322.
14. **Elliott DA, et al.** 2001. *Cryptosporidium parvum* infection requires host cell actin polymerization. Infect. Immun. **69**:5940–5942.
15. **Eto DS, Jones TA, Sundsbak JL, Mulvey MA.** 2007. Integrin-mediated host cell invasion by type 1-piliated uropathogenic *Escherichia coli.* PLoS Pathog. **3**:e100.
16. **Garrigues HJ, Rubinchikova YE, Dipersio CM, Rose TM.** 2008. Integrin alphaVbeta3 binds to the RGD motif of glycoprotein B of Kaposi's sarcoma-associated herpesvirus and functions as an RGD-dependent entry receptor. J. Virol. **82**:1570–1580.
17. **Gilcrease MZ.** 2007. Integrin signaling in epithelial cells. Cancer Lett. **247**:1–25.
18. **Harburger DS, Calderwood DA.** 2009. Integrin signalling at a glance. J. Cell Sci. **122**:159–163.
19. **Hynes RO.** 2004. The emergence of integrins: a personal and historical perspective. Matrix Biol. **23**:333–340.
20. **Hynes RO.** 2002. Integrins: bidirectional, allosteric signaling machines. Cell **110**:673–687.
21. **Isberg RR, Leong JM.** 1990. Multiple beta 1 chain integrins are receptors for invasin, a protein that promotes bacterial penetration into mammalian cells. Cell **60**:861–871.
22. **Kumar CC.** 1998. Signaling by integrin receptors. Oncogene **17**:1365–1373.
23. **Martin KH, Slack JK, Boerner SA, Martin CC, Parsons JT.** 2002. Integrin connections map: to infinity and beyond. Science **296**:1652–1653.
24. **Mitra SK, Schlaepfer DD.** 2006. Integrin-regulated FAK-Src signaling in normal and cancer cells. Curr. Opin. Cell Biol. **18**:516–523.
25. **Nesterenko MV, Upton SJ.** 1996. A rapid microcentrifuge procedure for purification of *Cryptosporidium* sporozoites. J. Microbiol. Methods **25**: 87–89.
26. **Petersen C, Barnes DA, Gousset L.** 1997. *Cryptosporidium parvum* GP900, a unique invasion protein. J. Eukaryot. Microbiol. **44**:89S–90S.
27. **Sanz-Moreno V, Marshall CJ.** 2010. The plasticity of cytoskeletal dynamics underlying neoplastic cell migration. Curr. Opin. Cell Biol. **22**:690–696.
28. **Takada Y, Ye X, Simon S.** 2007. The integrins. Genome Biol. **8**:215.
29. **Takagi J.** 2007. Structural basis for ligand recognition by integrins. Curr. Opin. Cell Biol. **19**:557–564.
30. **Templeton TJ, et al.** 2010. A genome-sequence survey for *Ascogregarina taiwanensis* supports evolutionary affiliation but metabolic diversity between a Gregarine and *Cryptosporidium.* Mol. Biol. Evol. **27**:235–248.
31. **Thompson RC, et al.** 2005. *Cryptosporidium* and cryptosporidiosis. Adv. Parasitol. **59**:77–158.
32. **Tzipori S, Ward H.** 2002. Cryptosporidiosis: biology, pathogenesis and disease. Microbes Infect. **4**:1047–1058.
33. **Untergasser A, et al.** 2007. Primer3Plus, an enhanced web interface to Primer3. Nucleic Acids Res. **35**:W71–W74.
34. **Xue Q, et al.** 2011. Entry of *Bacillus anthracis* spores into epithelial cells is mediated by the spore surface protein BclA, integrin alpha2beta1 and complement component C1q. Cell. Microbiol. **13**:620–634.
35. **Yan R, et al.** 2007. Aldo-keto reductase family 1 B10 gene silencing results in growth inhibition of colorectal cancer cells: implication for cancer intervention. Int. J. Cancer **121**:2301–2306.
36. **Zhu G, Keithly JS, Philippe H.** 2000. What is the phylogenetic position of *Cryptosporidium*? Int. J. Syst. Evol. Microbiol. **50**(Pt. 4):1673–1681.